Applied Catalysis B: Environmental 125 (2012) 95–102

Contents lists available at SciVerse ScienceDirect

Applied Catalysis B: Environmental

journal homepage: www.elsevier.com/locate/apcatb

Establishing the trichloroethene dechlorination rates of palladium-based catalysts and iron-based reductants

Shujing Li[a,b,d], Yu-Lun Fang[b], Chris D. Romanczuk[b], Zhaohui Jin[a], Tielong Li[a], Michael S. Wong[b,c,e,*]

[a] College of Environmental Science and Engineering, Nankai University, 94 Weijin Road, Tianjin, 300071, PR China
[b] Department of Chemical and Biomolecular Engineering, Rice University, 6100 Main Street, Houston, TX 77005, USA
[c] Department of Chemistry, Rice University, USA
[d] Tianjin Entry-Exit Inspection and Quarantine Bureau, No.8, Zhaofa New Zone, 2nd Street TEDA, Tianjin, 300457, PR China
[e] Department of Civil and Environmental Engineering, Rice University, USA

ARTICLE INFO

Article history:
Received 27 March 2012
Received in revised form 16 May 2012
Accepted 22 May 2012
Available online 30 May 2012

Keywords:
Trichloroethene
Iron
Palladium
Gold
Hydrodechlorination
Nanoparticles

ABSTRACT

The removal of undesired chlorinated hydrocarbon contaminants through chemical destruction using *ex situ* Pd-based catalytic or *in situ* Fe-based reductive nanomaterials offers unique advantages over current physical displacement methods for groundwater treatment. While these two types of chemical methods has been studied in-depth in recent years, their respective hydrodechlorination and dechlorination transformations have not been analyzed together before. Here, the reactivities of Pd catalysts and Fe reductants were experimentally assessed for trichloroethene (TCE) degradation using room-temperature, atmospheric-pressure, dihydrogen-headspace-filled batch reactor studies under buffered and non-buffered conditions. Pseudo-first order reaction rate constants at pH 7 spanned 9 decades: 1.2×10^4, 1.0×10^3, 4.5×10^2, 2.41×10^{-4}, 4.2×10^{-4}, and 7.09×10^{-6} $L/g_{active\text{-}metal}/min$ for Pd-on-Au nanoparticles (Pd/Au NPs), Pd NPs, Pd-on-alumina powder, and two nano-sized forms and one micron-sized form of commercial zerovalent iron, respectively. With rates measured in the range of commonly reported values, the Fe-based materials produced ethane, ethene, and vinyl chloride; ethene hydrogenated into ethane at sufficiently long reaction times. The much more active Pd-based materials produced ethane as the primary TCE degradation reaction product. This study presents, for the first time, a quantitative comparison of TCE degradation rates determined under identical experimental conditions.

1. Introduction

Chlorinated ethenes are a class of volatile organic compounds (VOCs) considered to being some of the most harmful of groundwater contaminants. These compounds have been linked to damage to livers, lungs, and the nervous system and developmental toxicity; and can cause death in humans with extreme exposure [1,2]. As a chlorinated ethene and a human carcinogen (as by the U.S. Environmental Protection Agency, EPA), trichloroethene (TCE) ranks 16th on the Comprehensive Environmental Response and Compensation Liability Act of 2007 (CERCLA) priority list of hazardous compounds [3]. From 1974 to 1984, over 100,000 tons of TCE per year was consumed in the US [4], mostly in the commercial and industrial sectors as a degreasing agent [2]. During 1998–2001, about ~0.45 tons of TCE was released to the environment [5]. According to a recent U.S. Geological Survey, 5% of groundwater sources known to be isolated from contaminant zones have been detected with TCE, with some sites detected with concentrations in excess of 200 ppb [2]. Additionally, 832 of 1430 National Priority List Superfund sites were detected with TCE at concentrations far above the U.S. EPA maximum contaminant level of 5 ppb (=5 μg/L = 0.038 μM) [6].

China is also experiencing issues with available clean water [7]. Used as a degreasing agent and in textile manufacture [8,9], TCE is consumed each year on the order of 50,000–60,000 tons [10]. TCE was recently detected in groundwater in some cities of China at extremely high concentrations (as high as 64,000 ppb [9]) much higher than the acceptable contaminant concentration limit of 70 ppb in drinking water set by the Ministry of Health of PR China [11] For comparison, the World Health Organization (WHO) recommends a drinking water limit of 20 ppb for TCE [12].

TCE is a highly persistent in groundwater, due to its continual release as a contaminant plume from subsurface deposits and its resistance to biotic and abiotic degradation mechanisms [13–15]. Whereas conventional TCE-contaminated groundwater treatment methods of air-stripping and carbon adsorption displace the offending compound from water, methods that degrade TCE

* Corresponding author at: Rice University, Chemical Engineering Dept, PO Box 1892, MS-362, Houston, TX 77251, United States. Tel.: +1 713 348 3511; fax: +1 713 348 5478.
E-mail address: mswong@rice.edu (M.S. Wong).

0926-3373/$ – see front matter © 2012 Elsevier B.V. All rights reserved.
http://dx.doi.org/10.1016/j.apcatb.2012.05.025

into a safer form continue to be sought. Bioremediation is a popular method to study for TCE degradation [16,17], but it suffers from low reaction rates and long clean-up times [18], and from the undesirable formation of partially dechlorinated TCE compounds like vinyl chloride [19].

More recent attention has been paid to a type of chemical treatment process, in which inorganic materials, specifically palladium (Pd)-based and iron (Fe)-based materials, are used for TCE degradation. These materials are similar in that they dechlorinate TCE into safer compounds at a faster rate compared to bioremediation, and the reactions are carried out under ambient conditions. The chemical transformation routes are very different, though.

The Pd materials are used as a catalyst, when a reducing agent like H_2 is present. They dechlorinate TCE into ethane; this transformation route is called catalytic hydrodechlorination (HDC). There is generally little to no formation of partially dechlorinated compounds, unlike bioremediation [20]. Different forms of Pd catalysts have been studied for the HDC of TCE and other chlorinated compounds, such as bimetallic Pd-on-Au nanoparticles (Pd/Au NPs), Pd nanoparticles (Pd NPs), and alumina-supported Pd (Pd/Al_2O_3) [21–24]. Pd/Au NPs are significantly more active [24–26] and more poison-resistant [1] than Pd NPs or Pd/Al_2O_3. Successful field demonstrations of Pd/Al_2O_3 and Pd/zeolite catalytic units are a promising sign towards a fully developed *ex situ* (above-ground) pump-and-treat technology [26–29].

In contrast, the Fe materials are used as a reducing agent. The chemical reactions that corrode Fe metal into rust can convert TCE into ethane, with partially dechlorinated TCE compounds occasionally being produced; this transformation route is called dechlorination. Commercially available Fe powder known as zero-valent iron (ZVI) is used in the field in permeable reactive barriers (PRB) as *in situ* (below-ground) groundwater treatment to manage the spread of TCE and other contaminants [30,31]. Other forms, such as nanostructured ZVI (nZVI) and Pd-doped ZVI, are being studied to extend capabilities of Fe [30,32–38]. nZVI was recently shown to be effective in the treatment of industrial wastewater in Shanghai, China [39].

There is ample evidence in literature that suggests that the reaction chemistry and reaction rates of these materials differ, but there are no studies that compare them side-by-side. In this work, we studied TCE degradation for Pd-based and Fe-based materials using the same reactor system and reaction conditions. We quantified Pd catalytic activities in terms of metal-content-normalized reaction rate constants and compared them to the reduction activities of nano-sized and non-nano-sized Fe powders. Clear and quantitative differences in reaction times, TCE degradation rates, and by-product formation emerged.

2. Experimental

2.1. Materials

Potassium carbonate (ACS reagent), tannic acid (ACS reagent), $PdCl_2$ (99.99%), trichloroethene (TCE, C_2HCl_3, 99.5%), Pd/Al_2O_3 (1 wt% Pd, powder), citric acid (ACS reagent, 99.5+%) and $HAuCl_4{\cdot}3H_2O$ (99.99%) from Sigma–Aldrich; trisodium citrate (99.5+%) from Fisher, and pentane (99.7%) from Burdick & Jackson were used as-received. Fe powder (H-200 Plus) was obtained from HEPURE Technologies Inc. [40], and two nanostructured Fe samples in slurry form (~20 wt%), NANOFER 25 and NANOFER 25S, were obtained from NANO IRON [41]. Deionized (DI) water (>18 MΩ cm) was produced using a Barnstead NANOpure Diamond system. Hydrogen gas (99.99%) was supplied by Matheson.

2.2. Preparation of Pd-based catalysts and Fe-based reductants

The preparation of Pd/Au NPs of one Pd surface coverage value and Pd NPs was carried out using our previous published methods [25]. Through aqueous-phase reduction, stable suspensions of Pd NPs (particle diameter = 4 nm, concentration = 1.22×10^{14} NP/L) and Pd/Au NPs (particle diameter = 4 nm, concentration = 1.07×10^{14} NP/L) were produced. The Pd/Au NPs were synthesized with a metal content of 6.8 wt% Pd and 93.2 wt% Au, which translated to NPs with a 30% monolayer coverage of Pd atoms. A suspension of Pd/Al_2O_3 was prepared by adding 0.0053 g of Pd/Al_2O_3 powder (1 wt% Pd, Sigma–Aldrich) into 3 mL of DI water, and ultrasonicated before use. Pd dispersion values for Pd/Au NPs, Pd NPs, and Pd/Al_2O_3 were ~100%, ~27%, and ~36%, respectively [26].

The Fe slurries were diluted prior to injection. They contained 20 wt% solid, of which 85% was Fe metal and the balance was Fe_3O_4, FeO, and C; the solid was in the form of agglomerated Fe nanoparticles (~50 nm) with a surface area of >25 m^2/g [41]. The particles of NANOFER 25 and NANOFER 25S contained a proprietary coating that reduced their pyrophoricity (Table 1).

2.3. Reaction studies

Batch experiments were similar to our previous studies [24] but modified to accommodate the use of the Fe materials. The batch reactor was prepared by adding 10 mL of a citrate buffer solution (5.8 mM) to ~159–162 mL of DI water in a 250-mL serum bottle, such that the resulting pH was 7.0. The citrate buffer solution was prepared by diluting 2.58 g of trisodium citrate into 100 mL DI water and then lowering the pH to 6.90 using 0.1 M citric acid (prepared by diluting 0.21 g of citric acid into 100 mL of DI water).

After being sealed with a cap outfitted with a rubber septum and Teflon tape, the bottle was bubbled with H_2 gas for 15 min to displace dissolved air from water and fill the headspace with H_2. Then, 1 μL of TCE and 0.5 μL of pentane (used as the internal standard for gas chromatography measurements) were injected into the bottle with a gas-tight syringe. It was then continuously agitated on a rocking platform (VWR, Model 100) at 40 oscillations/min. After gas chromatography measurements of the headspace indicated the TCE concentration became stable, a certain amount of the Pd- or Fe-based material was injected into the reactor to initiate the TCE dechlorination reaction (Table 1). The Fe powder (H-200 Plus sample) could not be injected through the rubber septum. Instead, it was placed in the bottle with the buffer solution prior to H_2 gas bubbling; any dechlorination activity was negligible due to its slow reactivity. The initial pH was ~7.0, and the initial TCE concentration was 8.5 ppm. The final reaction volume was 173 mL after adding the catalytic or reductant material. Non-buffered experiments were carried out by replacing the 10-mL buffer solution with 10-mL DI water. In control experiments, selected samples were carried out using an argon headspace instead of a H_2 headspace.

The reaction was carried out at room temperature (~22 °C) and atmospheric pressure, under continuous rocking. Reactor headspace samples (200 μL) were analyzed using an Agilent Technologies 6890 GC equipped with a flame ionization detector (FID) and a packed column (6-in. × 1/8-in. outer diameter) containing 60/80 Carbopack B/1% SP-1000 (Supelco). If TCE, the dichloroethene isomers (1,1-DCE, trans-1,2-DCE, cis-1,2-DCE), vinyl chloride (VC), ethane, ethane, and acetylene were detected, their concentrations were measured with reaction time.

Reaction rate constants for TCE (hydro)dechlorination were determined by assuming a pseudo-first-order TCE concentration dependence. At low TCE concentrations (like the value used in this study), this assumption is a valid one [42]. The H_2 content was in excess relative to TCE content; the maximum decrease

Table 1
Description of TCE dechlorination materials and amounts used per reactor.

Material tested	Final concentration of material in batch reactor	Description (sample amount charged to reactor)
Pd/Au NPs	2.44×10^{-5} g-Pd/L (3.0×10^{-4} g-Au/L)	Colloidal sol of 4-nm Au NPs with 30% ML Pd coverage; Pd dispersion ~ 100% (1 mL)
Pd NPs	1.77×10^{-4} g-Pd/L	Colloidal sol of ~4-nm Pd NPs; Pd dispersion ~27% (1 mL)
1 wt% Pd/Al_2O_3	3.1×10^{-4} g-Pd/L (3.1×10^{-2} g-solid/L)	Suspension containing 0.003 wt% powder in water; Pd dispersion ~36%; measured surface area ~200 m^2/g (3 mL)
NANOFER 25	5 g-Fe/L (29 g-solid/L)	Slurry containing 17 wt% Fe metal in water; agglomerated 50-nm particles with inorganic passivating agent; surface area ~25 m^2/g (3 mL)
NANOFER 25S	5 g-Fe/L (29 g-solid/L)	Slurry containing 17 wt% Fe metal in water; agglomerated 50-nm particles with organic passivating agent; surface area ~25 m^2/g (3 mL)
H-200 Plus	5.49 g-Fe/L (5.78 g-solid/L)	Powder containing particles < 250 microns; Fe metal content > 95%, surface area ~0.1 m^2/g (1 g)

in H_2 content is 2% at 100% TCE conversion). For Pd-based materials, $-dC_{TCE}/dt = k_{obs} \times C_{TCE}$, where the measured first-order rate constant is $k_{obs} = k_{Pd} \times C_{Pd}$ [24,25]. For Fe-based materials, $k_{obs} = k_{Fe} \times C_{Fe}$. The k_{Pd} and k_{Fe} are reaction rate constants normalized to total mass of Pd and Fe, respectively, with units of $L/g_{metal}/min$. C_{Pd} (or C_{Fe}) is the weight of Pd (or Fe) divided by the reaction fluid volume, and C_{TCE} is the TCE concentration in the bulk fluid.

3. Results and discussion

3.1. Comparison of dechlorination mechanisms

Using a Pd or Pd/Au catalyst, the dechlorination of TCE involves dihydrogen, *i.e.*, hydrodechlorination. Stoichiometically, this reaction is represented by the following chemical equation:

$$HClC{=}CCl_2 + 4H_2 \rightarrow H_3C{-}CH_3 + 3HCl \quad (1)$$

Mechanistically, it likely proceeds through a series of hydrogenolysis and hydrogenation steps, after activation of the dihydrogen and TCE on the catalyst surface (Fig. 1) [20,43,44]. Even though in-water surface-enhanced Raman spectroscopy results suggest the presence of a more complex set of surface reaction intermediates like π-bound and di-σ bound species and vinylidene species [45], the kinetics behavior can be captured with a classical Langmuir–Hinshelwood mechanism [42].

The reaction mechanism of TCE dechlorination by Fe materials is much more complicated, because of the loss of Fe metal during its corrosion, the interference of the iron hydroxides formed on the Fe surface, and the reaction of TCE on the Fe surface with *in situ* generated electrons and protons [14,46,47]. Nonetheless, the reaction can be represented stoichiometrically as:

$$HClC{=}CCl_2 + 4Fe^0 + 5H_2O \rightarrow H_3C{-}CH_3 + 4Fe^{2+} + 5OH^- + 3Cl^- \quad (2)$$

In the context of surface reactions, TCE dechlorination can occur on the Fe surface *via* a set of hydrogenolysis, hydrogenation and α-elimination (removal of 2 chloride atoms on the same carbon), and β-elimination (removal of chloride atoms on adjacent carbons) reaction steps, and propagated by the formation of adsorbed hydrogen species from the oxidation of iron. This process is depicted here as a set of surface-mediated surface reactions, with all the surface intermediates bound to the surface in non-specified binding configurations (Fig. 2). TCE dechlorination proceeds mostly through β-elimination followed by hydrogenation to form acetylene as a surface intermediate, as concluded by Arnold and Roberts [47]. Acetylene can be detected in solution [15,47,48] or not [15], depending on iron purity and reaction conditions.

3.2. Comparison of reaction rates

Tables 2 and 3 show the wide range of TCE dechlorination activities, respectively, as summarized from recent literature. The values were either drawn from the papers directly or calculated from the reported results. Reaction conditions of many of these studies differed or not indicated, making the comparison of rate data problematic. Different catalyst charge amounts and stir rates can change observed reaction rates, for example, which we quantitatively showed to be indicative of non-negligible mass transfer effects for catalyzed TCE hydrodechlorination [42]. The general observations are that high Pd dispersion and the presence of Au enhance the catalytic activity of Pd metal for TCE HDC, and that Fe-based materials are less active compared to Pd-based materials. Much more Fe material is needed for a TCE HDC reaction experiment, and the rate constants are smaller in value.

All Pd- and Fe-based materials were studied under buffered and non-buffered conditions in the same exact manner, *i.e.*, constant agitation, no magnetic stirring, H_2 headspace, room temperature, atmospheric pressure. A comparison of reaction rates from the non-buffered experiments revealed several notable findings (Table 4). The nanoparticulate forms of Fe, NANOFER 25 and NANOFER 25S, were much less active than the Pd-based materials, requiring ~10^4× more material (and more time) to produce observable changes in TCE concentration. Accounting for this mass difference, these were still at least 10^5× less active. The Fe powder (H-200 Plus) were ~100× less active than the nZVI materials on a mass basis, falling within the wide range of reported rate constants for the commercial and lab-prepared sources of nZVI (Table 3). Accounting for their estimated surface areas (Table 1), NANOFER 25, NANOFER 25S, and H-200 Plus samples had reaction rate constants of 1.16×10^{-5}, 7.52×10^{-6}, and 1.64×10^{-5} $L/m^2/min$, respectively. These Fe-based materials had comparable activity for TCE dechlorination on surface area basis.

Pd/Au NPs (with 30% Pd coverage) were more active (~22×) than Pd NPs or Pd/Al_2O_3 on a metal mass basis. The rate constants

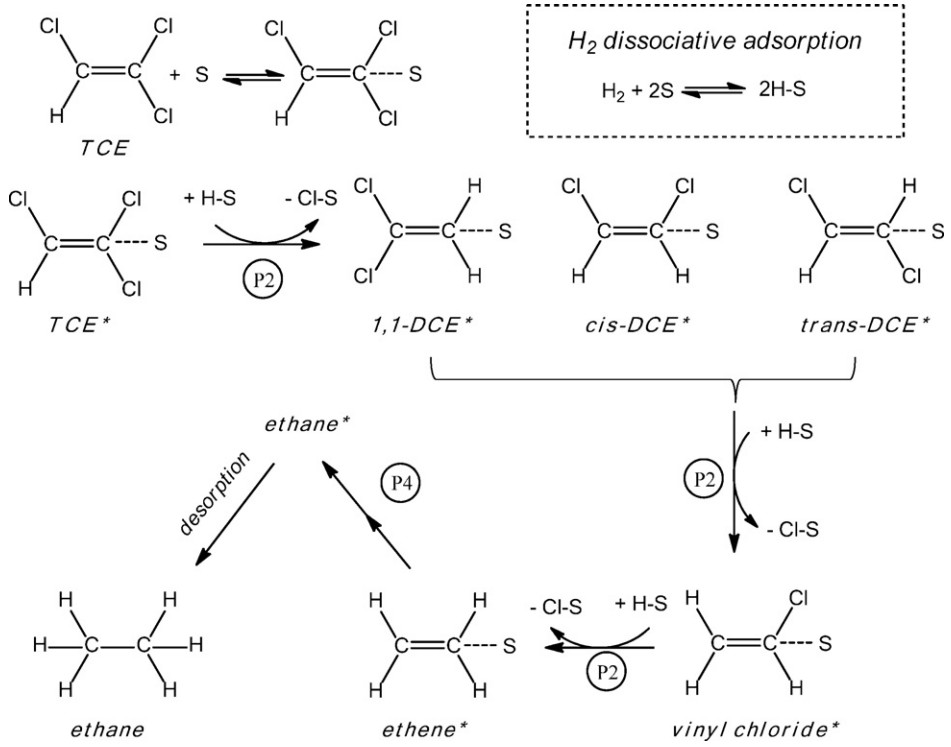

Fig. 1. Model of Pd- and Pd/Au-catalyzed TCE hydrodechlorination surface reaction. "S" represents an active site on the Pd or Pd/Au catalyst surface to which a chemical species is bound. The surface-bound species is designated with an asterisk (*). Surface reaction steps of hydrogenolysis (P2) and hydrogenation (P4) are indicated.

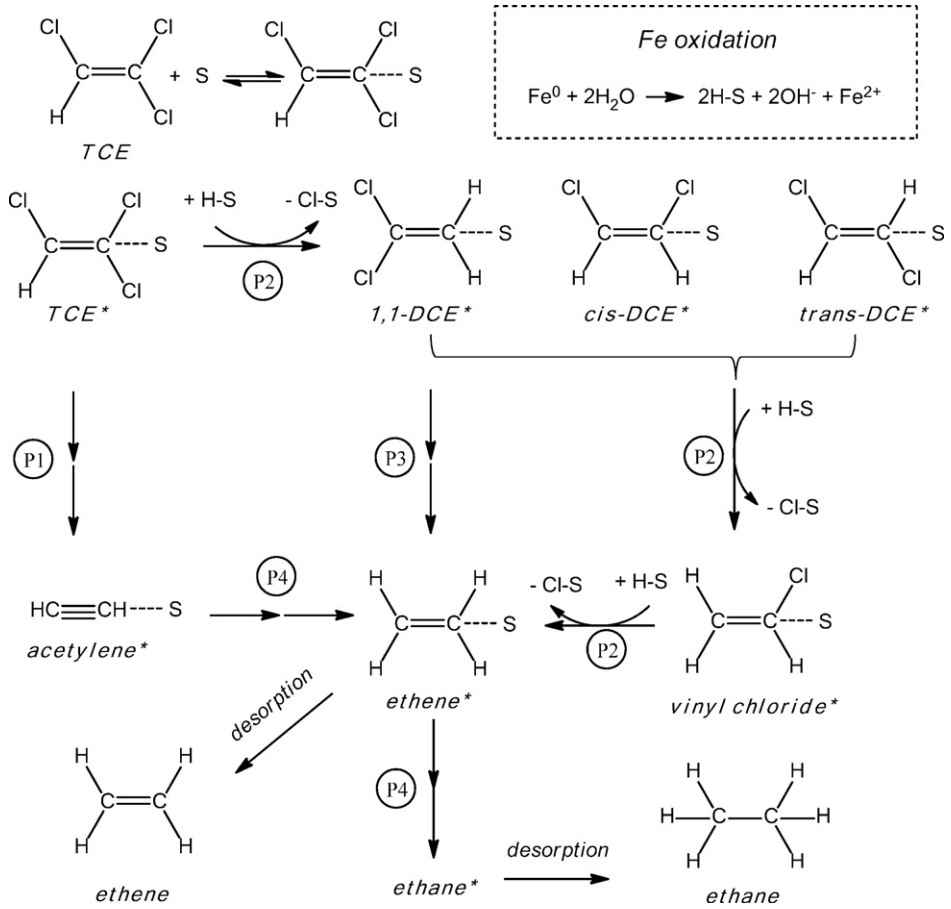

Fig. 2. Model of Fe-mediated TCE dechlorination surface reaction. "S" represents an active site on the Fe surface to which a chemical species is bound. The surface-bound species is designated with an asterisk (*). Surface reaction steps of β-elimination + hydrogenation (P1), hydrogenolysis (P2), α-elimination (P3), and hydrogenation (P4) are indicated.

Table 2
Literature data of pseudo-first-order reaction rate constants for TCE HDC with different types of Pd catalysts.

Catalyst type	Headspace gas	Metal content of reactor (g/L)	Initial [TCE] (ppm)	k_{obs} (min^{-1})[b]	k_{Pd} ($L/g_{Pd}/min$)	Initial pH	Buffer	Ref.
Pd/Al_2O_3 (0.5 wt% Pd)	H_2	0.125	20	16.125	139[b]	8.3	$NaHCO_3$ (5 mM)	Kopinke [49]
Pd/Al_2O_3 (1 wt% Pd)	H_2	1.45×10^{-3}	43	0.062	42.7	~7	n/a	Heck [1]
Pd/Au NPs (80% ML)	H_2	3.54×10^{-5}	60	0.081	2297	~7	n/a	Nutt [24]
Pd/Au NPs (60% ML)	H_2	1.15×10^{-5}	21.8	0.019	1630	~7	n/a	Fang [42]
Pd/Au NPs (60% ML)	H_2	1.15×10^{-5}	2.18	0.052	4560	~7	n/a	Fang [42]
Pd/Au NPs (30% ML)	H_2	4.43×10^{-5}	43	0.039	900	~7	n/a	Heck [1]
Pd NPs	H_2	1.77×10^{-4}	60	0.0097	55	~7	n/a	Nutt [24]
Pd/CMC[a]	H_2	0.0011	50	0.878	828	n/a	n/a	Liu [50]
Pd black	H_2	0.026	45.3	0.0109	0.42	~7	n/a	Nutt [25]

[a] 2.5-nm Pd NPs; CMC = carboxymethylcellulose coating on NPs.
[b] Re-calculated using published data.

Table 3
Literature data of pseudo-first-order reaction rate constants for TCE hydrodechlorination with different types of Fe reductants.

Reductant type	Headspace gas	Metal content of reactor (g/L)	Initial [TCE] (ppm)	k_{obs} (min^{-1})[c]	k_{Fe} ($L/g_{Fe}/min$)[c]	Initial pH	Buffer	Ref.
Fe NPs (30–40 nm)	Argon	1.9	4.4	1.62×10^{-2}	8.52×10^{-3}	n/a	None	Liu [15]
RNIP (Toda Kogyo Corp.)	Argon	1.9	4.4	2.26×10^{-3}	1.19×10^{-3}	n/a	None	Liu [15]
RNIP (Toda Kogyo Corp.)	Argon	2	3.55	3.67×10^{-4}	1.83×10^{-4}	7.0	HEPES[a]	Liu [51]
RNIP (Toda Kogyo Corp.)	Argon	2	14.46	4.00×10^{-4}	2.00×10^{-4}	7.0	HEPES[a]	Liu [51]
Fe^0 NPs	Air	20	20	3.35×10^{-2}	1.68×10^{-3}	n/a	None	Wang [52]
Fe^0 NPs	Argon	1.5	20	1.08×10^{-3}	7.21×10^{-4}	n/a	None	Li [53]
Fe^0 NPs	Argon	5	20	2.98×10^{-2}	5.95×10^{-3}	n/a	None	Li [53]
Fe (Hartgusstrahlmittel GH-R)	No headspace	130	n/a	3.73×10^{-4}	2.86×10^{-6}	n/a	None	Wust [54]
Fisher Fe^0 (100 mesh)	No Headspace	300	2	5.01×10^{-4}	1.67×10^{-6}	5.7	None	Su [55]
Master builders Fe^0	No Headspace	300	2	6.34×10^{-4}	2.11×10^{-6}	5.7	None	Su [55]
Peerless Fe^0	No Headspace	300	2	3.60×10^{-4}	1.20×10^{-6}	5.7	None	Su [55]
Aldrich Fe^0 (325 mesh)	No Headspace	300	2	3.07×10^{-6}	1.02×10^{-8}	5.7	None	Su [55]
Fisher Fe^0 (100 mesh)	No Headspace	1.562	1.578	1.83×10^{-4}	1.17×10^{-4}	7.2	Tris[b]	Arnold [47]
Fisher Fe^0 (100 mesh)	N/A	250	72	3.17×10^{-4}	1.27×10^{-6}	6.25	None	Gotpagar [56]
Commercial Fe powder (<10 μm)	Air	20	20	3.00×10^{-4}	1.50×10^{-5}	n/a	None	Wang [52]

[a] 50 mM 4-(2-hydroxyethyl)-1-piperazineethanesulfonic acid.
[b] 50 mM tris(hydroxymethyl)aminomethane + 0.5 M NaCl.
[c] Re-calculated using published data.

were higher than some other reported values as a result of lower initial TCE concentrations (Table 2) [42]. Accounting for Pd dispersion (Table 1), Pd/Au NPs, Pd NPs, and Pd/Al_2O_3 had estimated rate constants of 4450, 741, and 556 $L/g_{surface}Pd/min$, respectively.

The pH values decreased from ~7 to ~3 at the end of the Pd-based TCE hydrodechlorination reaction runs due to the proton generation (Eq. (1)) [55,57,58]. Performing the same reaction runs buffered at pH 7 yielded higher rate constants for all Pd materials by at least two times (Table 4). Acidic pH values have been observed to lower catalytic activity, consistent with electrochemical evidence of chloride ions adsorbing to Pd surfaces at low pHs [59]. Accounting for Pd dispersion, Pd/Au NPs, Pd NPs, and Pd/Al_2O_3 had estimated rate constants of 11900, 3704, and 1250 $L/g_{surfacePd}/min$, respectively. On a surface Pd atom basis, Pd/Au NPs were ~3 times more active than Pd NPs and ~10 times more active than Pd/Al_2O_3.

For Fe-based TCE dechlorination, the pH values increased from ~7 to ~9 at the end of the runs due to hydroxyl generation (Eq. (2)). Performing the reaction runs buffered at pH 7, too, yielded higher rate constants for all Fe materials, which was consistent with observations of lowered reactivity of micrometer-scale Fe powder and nZVI for TCE dechlorination at basic pH [58,60]. The extent of increase for the Fe-based materials was smaller than that for Pd-based catalysts (*cf.* 1.28× *vs.* 2×). Accounting for their estimated surface areas (Table 1), NANOFER 25, NANOFER 25S, and H-200 Plus samples had roughly comparable reaction rate constants of 1.68×10^{-5}, 9.64×10^{-6}, and 7.09×10^{-5} $L/m^2/min$, respectively.

Table 4
Experimental data of reaction rate constants for TCE HDC with different types of materials.

Material tested	Headspace gas	Metal content of reactor (g/L)	Initial [TCE] (ppm)	k_{obs} (min^{-1})	k_{Pd} or k_{Fe} ($L/g_{metal}/min$)	Initial pH	Buffer
Pd/Au NPs	H_2	2.44×10^{-5}	8.5	0.11 ± 0.01	4450 ± 150	~7.0	None
Pd NPs	H_2	1.77×10^{-4}	8.5	0.036 ± 0.001	200 ± 10	~7.0	None
Pd/Al_2O_3	H_2	3.1×10^{-4}	8.5	0.06 ± 0.01	200 ± 30	~7.0	None
NANOFER 25	H_2	5.00	8.5	0.0017	2.9×10^{-4}	~7.0	None
NANOFER 25S	H_2	5.00	8.5	0.0011	1.88×10^{-4}	~7.0	None
H-200 Plus	H_2	5.49	8.5	1×10^{-5}	1.64×10^{-6}	~7.0	None
Pd/Au NPs	H_2	2.44×10^{-5}	8.5	0.29 ± 0.03	11900 ± 1200	~7.0	0.1 M citrate
Pd NPs	H_2	1.77×10^{-4}	8.5	0.18 ± 0.02	1000 ± 200	~7.0	0.1 M citrate
Pd/Al_2O_3	H_2	3.1×10^{-4}	8.5	0.13 ± 0.01	450 ± 30	~7.0	0.1 M citrate
NANOFER 25	H_2	5.00	8.5	0.0024	4.2×10^{-4}	~7.0	0.1 M citrate
NANOFER 25S	H_2	5.00	8.5	0.0014	2.41×10^{-4}	~7.0	0.1 M citrate
H-200 Plus	H_2	5.49	8.5	4.33×10^{-5}	7.09×10^{-6}	~7.0	0.1 M citrate

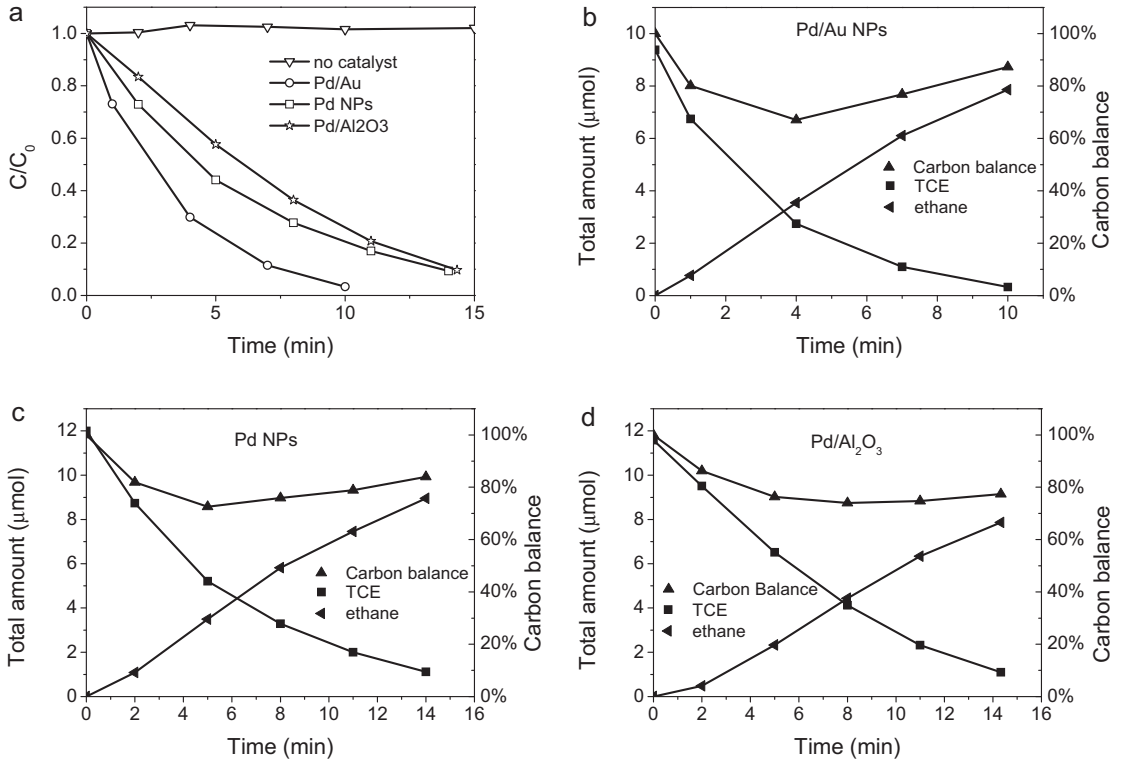

Fig. 3. (a) Normalized TCE concentration profiles in water for Pd-based catalysts for TCE HDC. Time profiles of total amount of detected species and carbon mole balance for (b) Pd/Au NPs, (c) Pd NPs, and (d) Pd/Al_2O_3. Initial TCE concentration in water (buffered at pH 7) = 8.5 ppm.

The small values of TCE degradation rates are attributed in part to iron hydroxide formation during iron oxidation [55,57,58].

3.3. Reaction selectivity

TCE concentrations decreased to <10% of initial concentration by 15 min for all forms of the Pd catalysts (Fig. 3a). TCE concentration decrease was not observed in the absence of a catalyst, indicating no leakage of TCE from the sealed serum bottle under constant rocking. Ethane was the sole reaction product detected; the partially chlorinated products VC or the DCE isomers, ethene, and acetylene were not detected. Calculated as the total gas-phase and water-phase amounts of detectible species (TCE and ethane) divided by initial TCE amount, the carbon balance for the Pd/Au NP-catalyzed reaction dropped to 67% before recovering to 87% (Fig. 3b). Pd NPs and Pd/Al_2O_3 catalysts led to carbon mass balances that decreased to ~73% before increasing to 84% and 77%, respectively (Fig. 3c and d). The temporal change in carbon balances suggested the adsorption of reaction intermediates that eventually converted into ethane. The non-closure of the carbon balances at the end of the reaction runs could be due to incomplete desorption of reaction intermediates, the formation of non-volatile products, and/or the formation of butenes/butanes (which were observed in a previous report [24] but were not targeted for GC measurements in this study).

TCE concentrations decreased to <10% of initial concentration after ~25 h for the nanosized Fe materials, and after ~250 h for the micron-sized Fe (Fig. 4a). There was negligible leakage of TCE from the batch reactor for at least 300 h. Ethane, ethene, and VC were detected as the main reaction products; no DCE isomers were detected, consistent with literature [15]. Acetylene was not detected. With the nanosized Fe materials, the carbon balance (calculated as the total gas-phase and water-phase amounts of ethane, ethene, VC, and TCE divided by initial TCE amount) decreased from 100% initially to 60–70% and increased back to 100%, indicating that any adsorbed reaction intermediate eventually converted and desorbed as a detectible species (Fig. 4b and c). Ethene accumulated substantially during the reaction, exceeding ethane concentration. The loss of ethene coupled with the increase in ethane concentration indicated Fe-surface-mediated ethene adsorption and hydrogenation occurred, even after complete consumption of TCE. VC slowly accumulated also, but to a smaller extent, consistent with observed difficulties of Fe in dechlorinating VC [48].

The less reactive micron-sized Fe reached a carbon mole balance of only ~70%, which was attributed to reaction products that were not measured in this study, *e.g.*, butenes and butanes and also propene/propane and 5-carbon and 6-carbon compounds as detected by others (Fig. 4d) [15]. Ethane, ethene, and VC accumulated throughout the reaction run. That ethene did not decrease in concentration was a significant difference from the nano-Fe forms. While the dechlorination activity were roughly similar for all 3 samples on a surface area basis, the surface sites on bulk Fe were unable to promote ethene hydrogenation that was observed for the nano-Fe forms.

A comparison of detected (hydro)dechlorination products at different TCE conversions using Pd-based catalysts and Fe-based reductants highlighted the differences between the two types of materials (Table 5). At 50% TCE conversion, all Pd-based catalysts gave 100% selectivity to ethane, the fully dechlorinated and hydrogenated product, and the Fe-based reductants yielded ~32–35% selectivity to ethane. The nano Fe forms yielded more ethene (63–65%) than micron-sized Fe (57%), with the latter giving substantially more VC. At longer reaction times to reach 90% TCE conversion, the relative amounts of ethane and VC increased for the Fe-based reductants. At the end of the reaction runs, the relative amounts of ethane and VC further increased for the nano-forms of Fe, though not for the micron form.

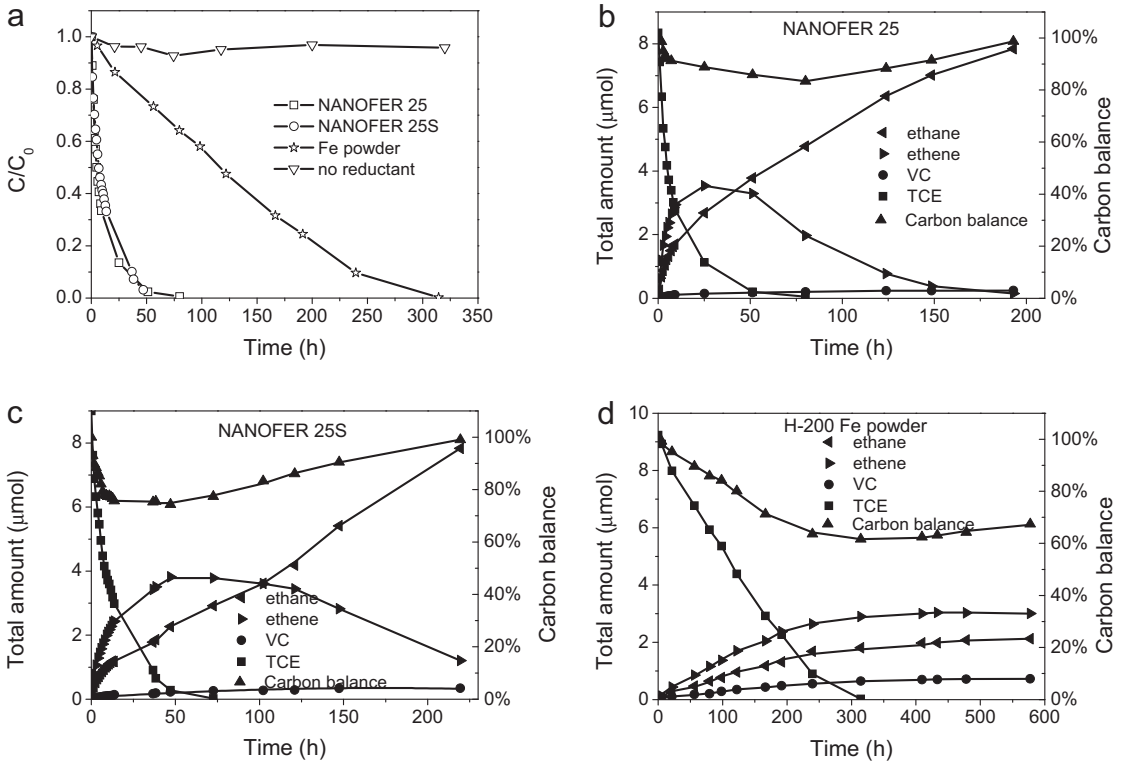

Fig. 4. (a) Normalized TCE concentration profiles in water for Fe-based reductants for TCE dechlorination. Time profiles of total amount of detected species and carbon mole balance for (b) NANOFER 25, (c) NANOFER 25S, and (d) H-200 Plus. Initial TCE concentration in water (buffered at pH 7) = 8.5 ppm.

Table 5
Product selectivities at different TCE conversions.[a]

Material tested	50% TCE conversion			90% TCE conversion			End of reaction run[b]		
	S_{VC} (%)	S_{ethene} (%)	S_{ethane} (%)	S_{VC} (%)	S_{ethene} (%)	S_{ethane} (%)	S_{VC} (%)	S_{ethene} (%)	S_{ethane} (%)
Pd/Au NPs	0	0	100	0	0	100	0	0	100
Pd NPs	0	0	100	0	0	100	0	0	100
Pd/Al_2O_3	0	0	100	0	0	100	0	0	100
NANOFER 25	1.7	63.4	34.9	2.3	55.6	42.1	2.9	1.8	95.2
NANOFER 25S	3.1	64.5	32.4	3.2	63.7	33.1	3.7	12.9	83.5
H-200 Plus	11.6	56.5	31.9	11.3	54.2	34.5	12.4	51.3	36.3

[a] Product selectivity values were calculated as total amount of the specific chemical species divided by the total amount of VC, ethene, and ethane formed. DCE's and acetylene were not formed. For some materials, the sum of the selectivity values exceeded 100% due to rounding errors.
[b] Calculated for the last time point for each material shown in Figs. 3 and 4.

4. Conclusions

The water-phase TCE degradation properties of Pd catalysts and Fe reductants were compared and quantitatively assessed under identical reaction conditions, specifically at room temperature, atmospheric pressure, pH 7, and low TCE concentration with constant agitation, no magnetic stirring, and H_2 headspace. All Pd-based catalysts showed high TCE degradation activity (on the order of minutes). Au metal caused Pd metal to be ~22× more active than Pd NPs and Pd/Al_2O_3 on a total Pd atom basis (or, counting only surface Pd atoms, 6× and 8× more active). All Fe-based reductants showed low TCE degradation activity (on the order of 10's of hours), with the 2 nano-sized forms of Fe being more active than micron-sized Fe due to their higher surface areas. The pH of the reaction medium decreased during Pd catalysis and increased during Fe reduction, leading to decreased degradation activity as reported by others. By buffering the reaction at pH 7, overall higher reaction rate constants resulted for all materials. Pd/Au NPs were 12× and 26× more active than Pd NPs and Pd/Al_2O_3 on a total Pd atom basis, respectively (or, on a surface Pd atom basis, 3× and 10× more active).

The Pd-based catalysts produced exclusively ethane as the TCE degradation product, whereas the Fe-based reductants produced ethene and VC in addition to ethane. The differences in activity and selectivity may be attributed to a material's ability to form surface H atoms. Pd-based catalysts readily activate H_2 through dissociative adsorption on the Pd metal, whereas Fe-based materials do not. Instead they form surface H atoms through Fe metal oxidation, a process that is kinetically slower than H_2 activation and one that generates surface-bound iron hydroxides. These results highlight the two roles that Pd may play in Pd-coated Fe materials, which have been studied by a number of groups for TCE HDC and other reactions [38,61,62]. In these materials, Pd metal can catalyze TCE HDC and it can accelerate the formation of surface H atoms, consistent with the observed higher degradation rates and smaller amounts of VC and ethene products.

On a metal mass basis, Pd/Au NPs were 9 orders of magnitude more active than the least active form of Fe, suggesting an

overwhelming case for using reductive catalysis to treat groundwater contamination. From the perspective of economics, however, the long-term costs of a cleanup operation need to be considered with the materials costs. Davie et al. [29] analyzed the costs of treating TCE-contaminated groundwater using Pd reductive catalysis and Fe-based PRB (as well as air-stripping and carbon adsorption). Using field-test results and extrapolating the costs over a ten-year period, they found that the Pd catalysis approach was at least 20× less costly than the PRB approach. Even though Pd metal is much more expensive, the large amounts of Fe material and the need for its replenishing outweigh the equipment, operational, and catalyst regeneration costs of a Pd/Al_2O_3-based reactor unit. With the Pd/Au NPs being at least 10× more active than Pd/Al_2O_3, a Pd/Au-based catalysis approach is expected to be less costly than the Pd/Al_2O_3-based and Fe-based approaches.

Acknowledgments

This work was supported by the Welch Foundation (C-1676) and the National Science Foundation (CBEN, EEC-0647452). We are grateful to the China Scholarship Council for financial support, and to the companies HEPURE Technologies Inc. (USA) and NANO IRON, s.r.o. (Czech Republic) for generously providing the iron samples for this study.

Appendix A. Supplementary data

Supplementary data associated with this article can be found, in the online version, at http://dx.doi.org/10.1016/j.apcatb.2012.05.025.

References

[1] K.N. Heck, M.O. Nutt, P. Alvarez, M.S. Wong, Journal of Catalysis 267 (2009) 97–104.
[2] M.J. Moran, J.S. Zogorski, P.J. Squillace, Environmental Science & Technology 41 (2007) 74–81.
[3] CERCLA priority list of hazardous substances, Agency for toxic substances and disease registry-US department of health and human services, 2007.
[4] Proposed identification of trichloroethylene as a toxic air contaminant, California Air Resources Board and the Department of Health Service, 1990.
[5] 2001 Toxics Release Inventory Public Data Release Report, U.S. Environmental Protection Agency, Washington DC, 2003.
[6] 2004 edition National Primary Drinking Water Regulations, 2004 ed., U.S. United States Environmental Protection Agency, 2004.
[7] C. Yu, Nature 470 (2011) 307.
[8] J.T. He, Y. Li, S. Liu, H.H. Chen, Environmental Science 26 (2005) 5.
[9] B. Han, J.T. He, H.H. Chen, H.W. Zhan, J.H. Shi, Earth Science Frontiers 13 (2006) 224–229.
[10] Y. Zheng, Y. Dai, China Occupational Medicine 33 (2006) 388–390.
[11] http://www.moh.gov.cn/publicfiles//business/htmlfiles/wsb/index.htm.
[12] http://www.who.int/water_sanitation_health/dwq/GDWAN4rev1and2.pdf.
[13] P.J. Squillace, M.J. Moran, W.W. Lapham, C.V. Price, R.M. Clawges, J.S. Zogorski, Environmental Science & Technology 33 (1999) 4176–4187.
[14] W.S. Orth, R.W. Gillham, Environmental Science & Technology 30 (1996) 66–71.
[15] Y.Q. Liu, S.A. Majetich, R.D. Tilton, D.S. Sholl, G.V. Lowry, Environmental Science & Technology 39 (2005) 1338–1345.
[16] A.K. Shukla, P. Vishwakarma, S.N. Upadhyay, A.K. Tripathi, H.C. Prasana, S.K. Dubey, Bioresource Technology 100 (2009) 2469–2474.
[17] M.A. Widdowson, Biodegradation 15 (2004) 435–451.
[18] Z.M. Xiu, Z.H. Jin, T.L. Li, S. Mahendra, G.V. Lowry, P.J.J. Alvarez, Bioresource Technology 101 (2010) 1141–1146.
[19] B.K. Amos, R.C. Daprato, J.B. Hughes, K.D. Pennell, F.E. Loffler, Environmental Science & Technology 41 (2007) 1710–1716.
[20] G.V. Lowry, M. Reinhard, Environmental Science & Technology 33 (1999) 1905–1910.
[21] C.G. Schreier, M. Reinhard, Chemosphere 31 (1995) 3475–3487.
[22] G.V. Lowry, M. Reinhard, Environmental Science & Technology 35 (2001) 696–702.
[23] D. Angeles-Wedler, K. MacKenzie, F.D. Kopinke, Environmental Science & Technology 42 (2008) 5734–5739.
[24] M.O. Nutt, K.N. Heck, P. Alvarez, M.S. Wong, Applied Catalysis B-Environmental 69 (2006) 115–125.
[25] M.O. Nutt, J.B. Hughes, M.S. Wong, Environmental Science & Technology 39 (2005) 1346–1353.
[26] Y.L. Fang, J.T. Miller, N. Guo, K.N. Heck, P.J.J. Alvarez, M.S. Wong, Catalysis Today 160 (2011) 96–102.
[27] C. Schuth, N.A. Kummer, C. Weidenthaler, H. Schad, Applied Catalysis B-Environmental 52 (2004) 197–203.
[28] W.W. McNab, R. Ruiz, M. Reinhard, Environmental Science & Technology 34 (2000) 149–153.
[29] M.G. Davie, H.F. Cheng, G.D. Hopkins, C.A. Lebron, M. Reinhard, Environmental Science & Technology 42 (2008) 8908–8915.
[30] Y.T. He, J.T. Wilson, R.T. Wilkin, Environmental Science & Technology 42 (2008) 6690–6696.
[31] D.H. Phillips, T. Van Nooten, L. Bastiaens, M.I. Russell, K. Dickson, S. Plant, J.M.E. Ahad, T. Newton, T. Elliot, R.M. Kalin, Environmental Science & Technology 44 (2010) 3861–3869.
[32] S.J. Li, T.L. Li, Z.M. Xiu, Z.H. Jin, Journal of Environmental Monitoring 12 (2010) 1153–1158.
[33] B. Flury, J. Frommer, U. Eggenberger, U. Mader, M. Nachtegaal, R. Kretzschmar, Environmental Science & Technology 43 (2009) 6786–6792.
[34] W. Wang, Z.H. Jin, T.L. Li, H. Zhang, S. Gao, Chemosphere 65 (2006) 1396–1404.
[35] B.W. Zhu, T.T. Lim, J. Feng, Environmental Science & Technology 42 (2008) 4513–4519.
[36] R. Muftikian, K. Nebesny, Q. Fernando, N. Korte, Environmental Science & Technology 30 (1996) 3593–3596.
[37] C. Grittini, M. Malcomson, Q. Fernando, N. Korte, Environmental Science & Technology 29 (1995) 2898–2900.
[38] W.X. Zhang, C.B. Wang, H.L. Lien, Catalysis Today 40 (1998) 387–395.
[39] L.M. Ma, W.X. Zhang, Environmental Science & Technology 42 (2008) 5384–5389.
[40] http://www.hepure.com/.
[41] http://www.nanoiron.cz/.
[42] Y.L. Fang, K.N. Heck, P.J.J. Alvarez, M.S. Wong, ACS Catalysis 1 (2011) 128–138.
[43] F.D. Kopinke, K. Mackenzie, R. Koehler, A. Georgi, Applied Catalysis A-General 271 (2004) 119–128.
[44] M.S. Wong, P.J.J. Alvarez, Y.L. Fang, N. Akcin, M.O. Nutt, J.T. Miller, K.N. Heck, Journal of Chemical Technology and Biotechnology 84 (2009) 158–166.
[45] K.N. Heck, B.G. Janesko, G.E. Scuseria, N.J. Halas, M.S. Wong, Journal of the American Chemical Society 130 (2008) 16592–16600.
[46] A.L. Roberts, L.A. Totten, W.A. Arnold, D.R. Burris, T.J. Campbell, Environmental Science & Technology 30 (1996) 2654–2659.
[47] W.A. Arnold, A.L. Roberts, Environmental Science & Technology 34 (2000) 1794–1805.
[48] J. Hara, H. Ito, K. Suto, C. Inoue, T. Chida, Water Research 39 (2005) 1165–1173.
[49] F.D. Kopinke, D. Angeles-Wedler, D. Fritsch, K. Mackenzie, Applied Catalysis B-Environmental 96 (2010) 323–328.
[50] J.C. Liu, F. He, E. Durham, D.Y. Zhao, C.B. Roberts, Langmuir 24 (2008) 328–336.
[51] Y. Liu, T. Phenrat, G.V. Lowry, Environmental Science & Technology 41 (2007) 7881–7887.
[52] C.B. Wang, W.X. Zhang, Environmental Science & Technology 31 (1997) 2154–2156.
[53] F. Li, C. Vipulanandan, K.K. Mohanty, Colloids and Surfaces A-Physicochemical and Engineering Aspects 223 (2003) 103–112.
[54] W.F. Wust, R. Kober, O. Schlicker, A. Dahmke, Environmental Science & Technology 33 (1999) 4304–4309.
[55] C.M. Su, R.W. Puls, Environmental Science & Technology 33 (1999) 163–168.
[56] J. Gotpagar, S. Lyuksyutov, R. Cohn, E. Grulke, D. Bhattacharyya, Langmuir 15 (1999) 8412–8420.
[57] Y.Q. Liu, H. Choi, D. Dionysiou, G.V. Lowry, Chemistry of Materials 17 (2005) 5315–5322.
[58] Y.Q. Liu, G.V. Lowry, Environmental Science & Technology 40 (2006) 6085–6090.
[59] A. Carrasquillo, J.J. Jeng, R.J. Barriga, W.F. Temesghen, M.P. Soriaga, Inorganica Chimica Acta 255 (1997) 249–254.
[60] M.L. Tamara, E.C. Butler, Environmental Science & Technology 38 (2004) 1866–1876.
[61] F. He, D.Y. Zhao, Environmental Science & Technology 39 (2005) 3314–3320.
[62] D.W. Elliott, W.X. Zhang, Environmental Science & Technology 35 (2001) 4922–4926.